

Electronic Supplementary Information

Two Cyclohexane-type Octadecanuclear metalla-macrocycle-based Metal Organic Frameworks and Adsorption Properties

Shufang Chen^a, Jiyong Hu^a, Jin'an Zhao^{a,*}, Jin Zhang^b, Huaibin Yu^b, Shuangcheng Zhi^b, Junshuai Zhang^a and Zhanqiang Gong^a

^aCollege of Chemical and Material Engineering, Henan University of Urban Construction, Henan 467036, P.R. China, and ^bCollege of Chemistry and Molecular Engineering, Zhengzhou University, Zhengzhou, 450052, Henan, P.R. China

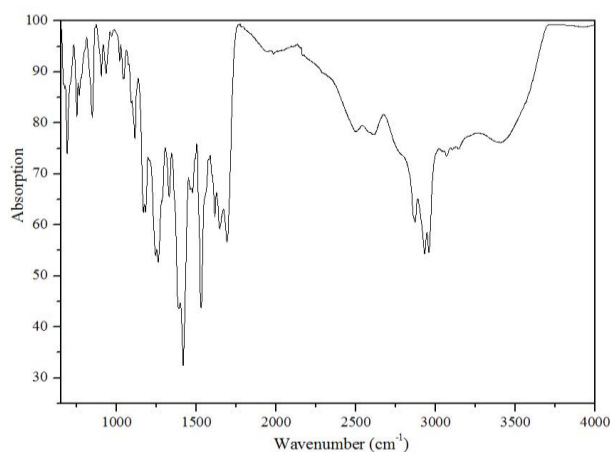


Figure S1. IR spectrum of sample 1.

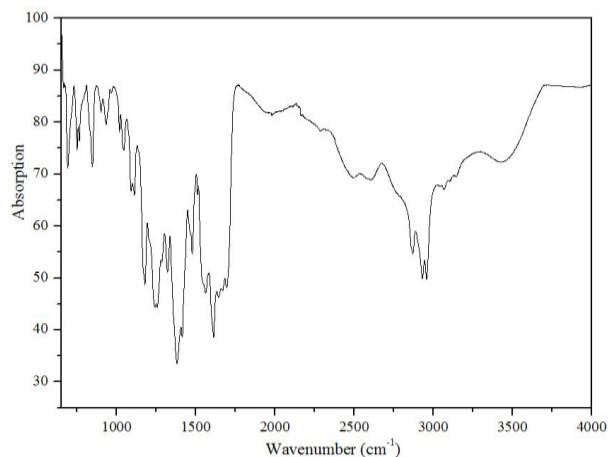


Figure S2. IR spectrum of sample 2.

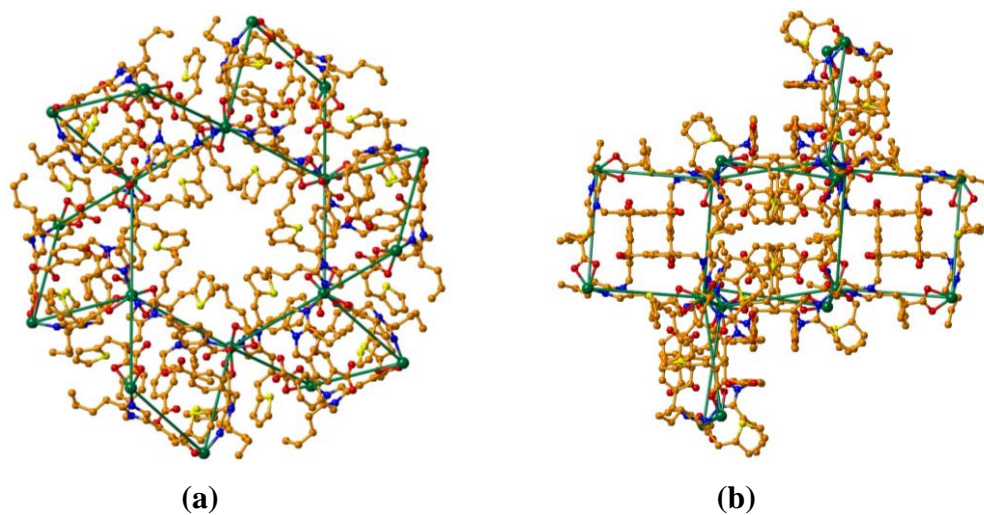


Figure. S3. A view of octadecanuclear Ni(II) aggregate along crystallographic [1,1,1] (a) axis and a axis (b), respectively.

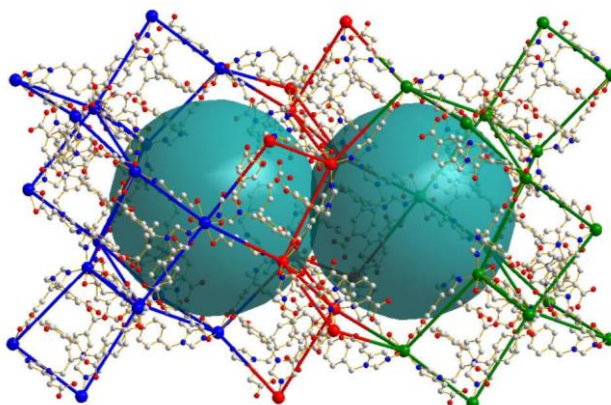


Figure. S4. Detail of the cavity between two octadecanuclear aggregate along crystallographic [1,1,1] axis (solvent molecules and ligands have been omitted for clarity).

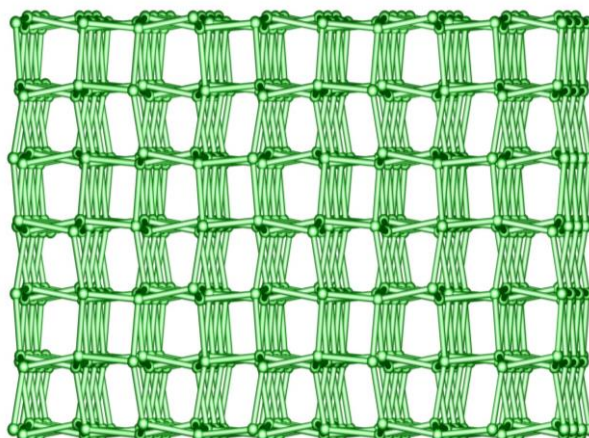


Figure. S5. Schematic representation of the 4-connected 3D network of **1** with $4^2.6^2.8^2$ topology.

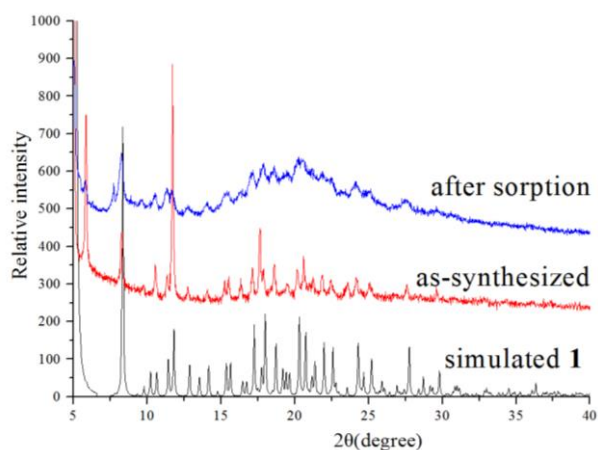


Figure S6. Powder X-ray diffraction (PXRD) patterns of **1** simulated from X-ray single-crystal data (bottom), and experimental data (top).

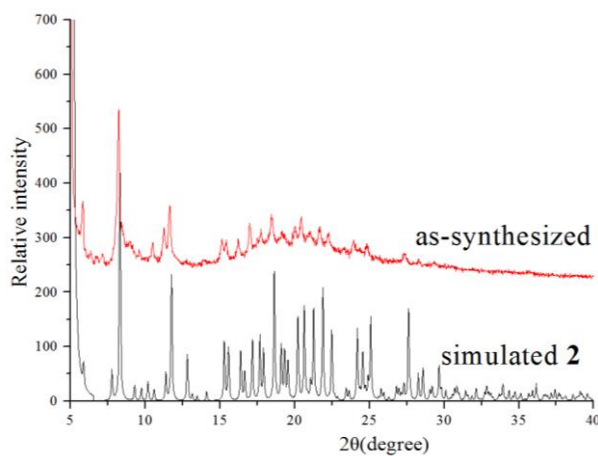


Figure S7. Powder X-ray diffraction (PXRD) patterns of **2**.

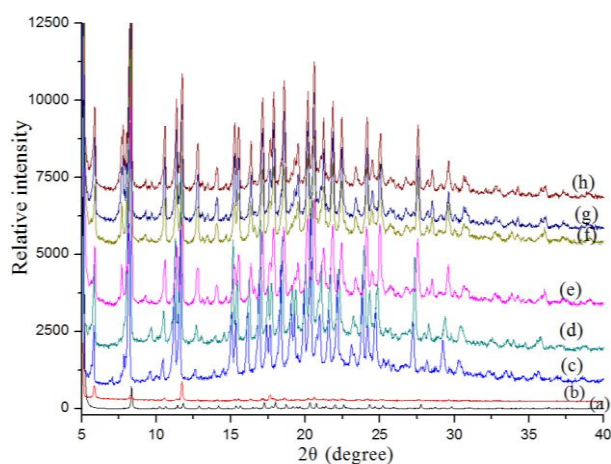


Figure S8. PXRD patterns of **1** with distinct conditions: (a) simulated pattern; (b) as-synthesized pattern; (c) immersed **1** in DMF for six hours; (d) immersed **1** in DMF for twelve hours; (e) immersed **1** in DMF for twenty-four hours; (f) prepared by soaking **1** in methanol for six hours; (g) prepared by soaking **1** in methanol for twelve hours; (h) prepared by soaking **1** in methanol for twenty-four hours.

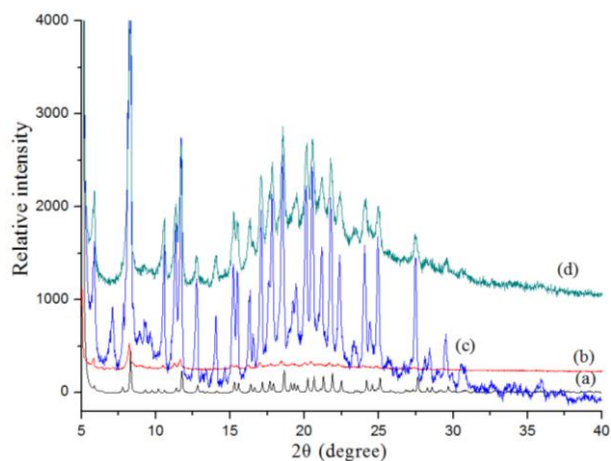


Figure S9. PXRD patterns of **2** under varied conditions: (a) simulated pattern; (b) as-synthesized pattern; (c) immersed **2** in methanol for six hours; (d) prepared by soaking **2** in methanol for twelve hours.

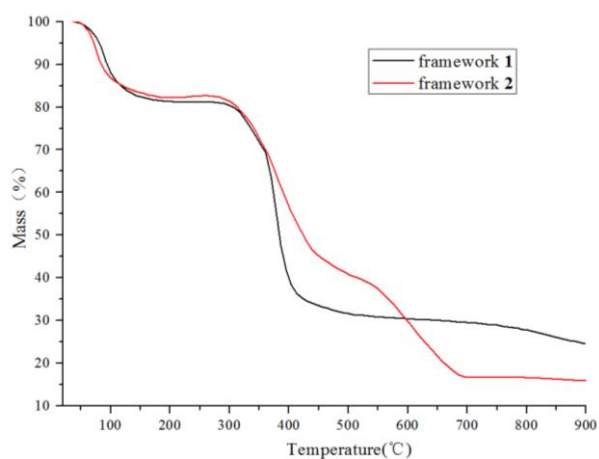


Figure. S10. Thermogravimetric analyses (TGA) curves for frameworks **1** and **2**.

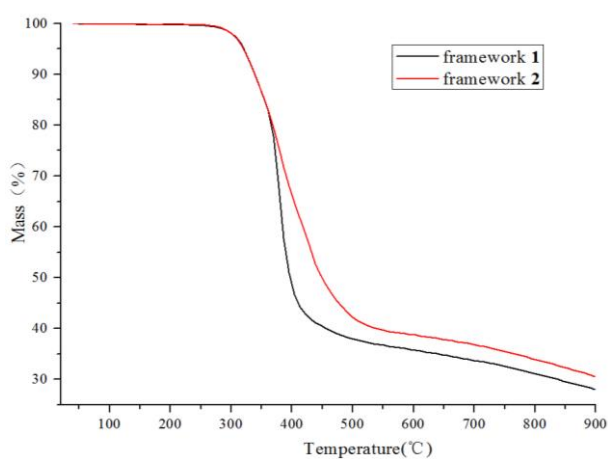


Figure. S11. Thermogravimetric analyses (TGA) curves for desolvated frameworks **1** and **2**.

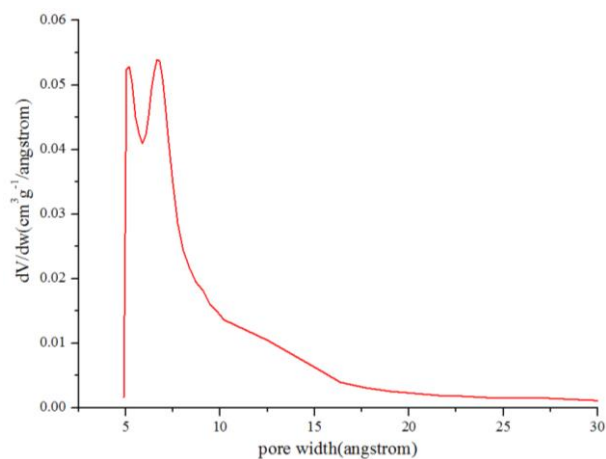


Figure. S12. Horvath-Kawazoe pore size distribution plot of complex 1.

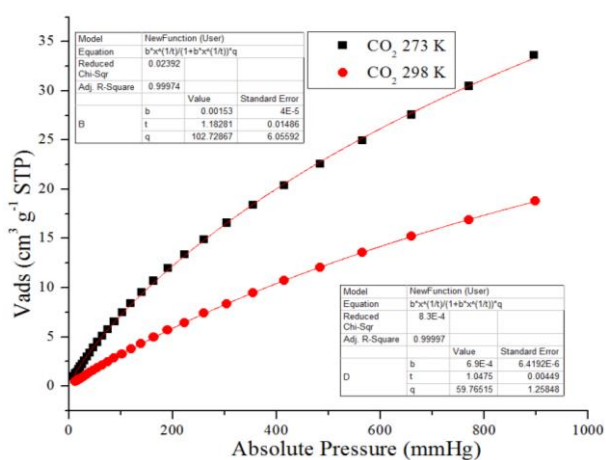


Figure S13. Fitting CO₂ adsorption isotherms using the Langmuir-Freundlich equation.

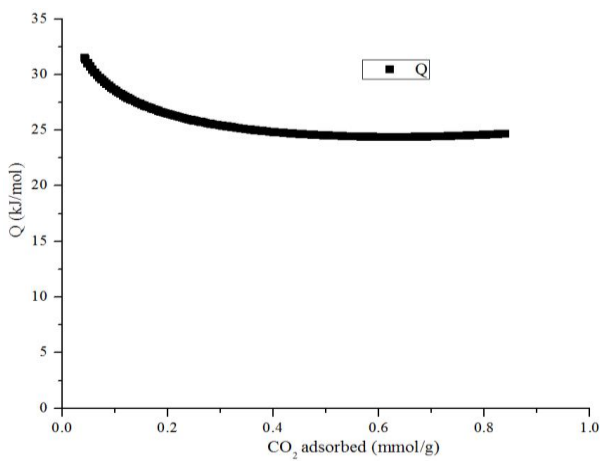


Figure S14. Isosteric heat of CO₂ adsorption.

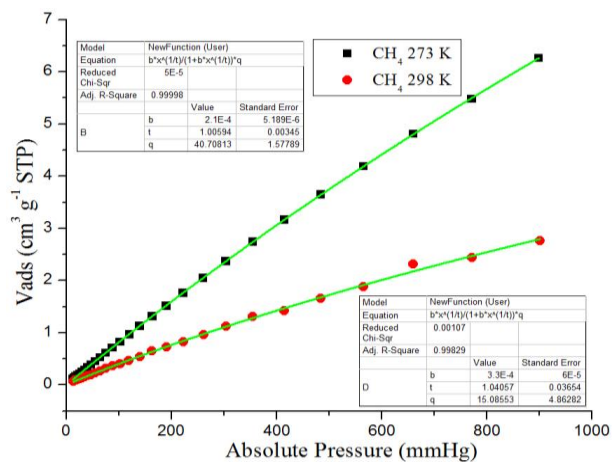


Figure S15. Fitting CH₄ adsorption isotherms using the Langmuir-Freundlich equation.

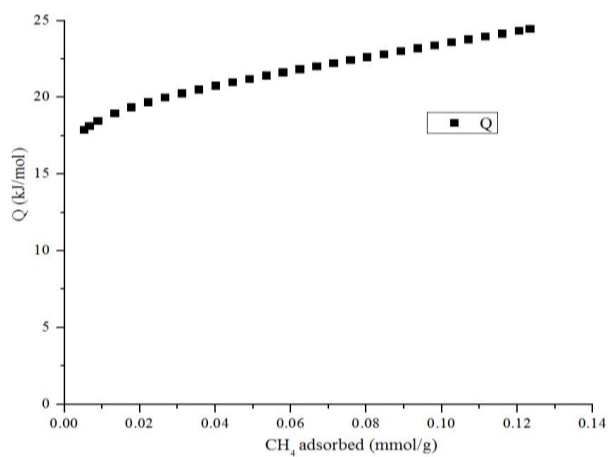
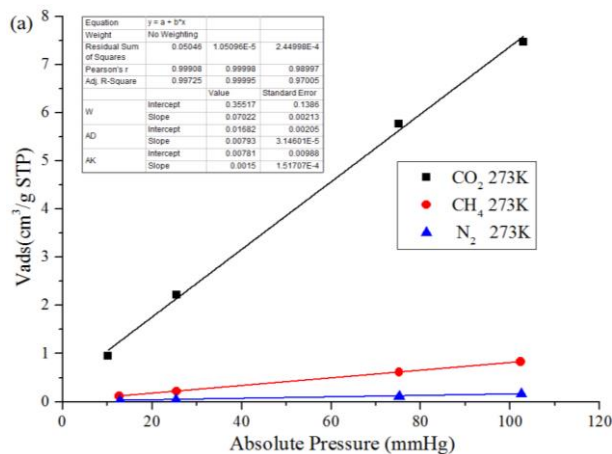


Figure S16. Isosteric heat of CH₄ adsorption.



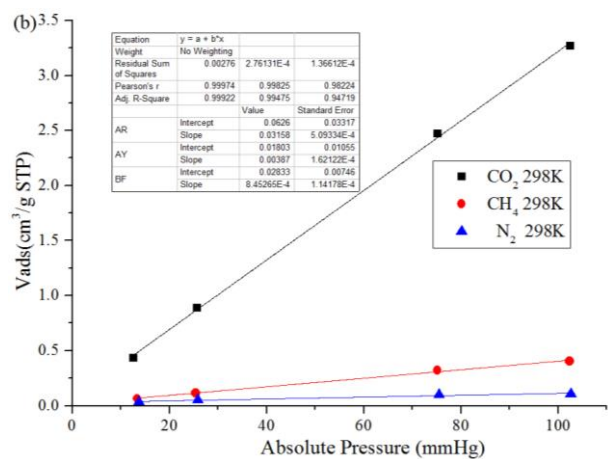


Figure S17. The fitting initial slopes of CO₂, CH₄ and N₂ of framework 1 at 273 K (a) and 298 K (b).

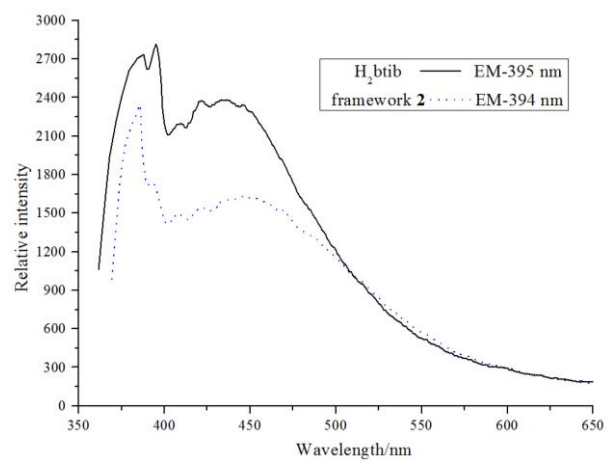


Figure. S18. Emission spectra of H₂btib and framework 2 in the solid state at room temperature.